

Solution and Solid State Structure of a Canted, Side-to-Face, Bis(porphyrin) Adduct

Enzo Alessio,^{*,†} Silvano Geremia,[†] Stefano Mestroni,[†] Elisabetta Iengo,[†] Ivana Srnova,^{†,‡} and Miroslav Slouf[§]

Dipartimento di Scienze Chimiche, Università di Trieste, 34127 Trieste, Italy, and Sincrotrone Trieste SpA, Trieste, Italy

Received July 14, 1998

The coordination chemistry of *meso*-pyridyl/phenyl porphyrins (PyPs) toward metallo-porphyrins with substitutionally labile axial ligands has been exploited for the self-assembling of ordered arrays of pigments. PyPs are particularly versatile building blocks: the peripheral N atom can be either in the 4'-position (4'PyPs) or in the 3'-position (3'PyPs), and they can provide connections to as many as four metal centers by coordination of the pyridyl groups. While 4'PyPs lead to arrays of perpendicularly linked, side-to-face, porphyrins, 3'PyPs yield the corresponding canted analogues. Even though several perpendicular arrays have been described, the examples of canted adducts are few and all very recent. We report here a detailed X-ray structure of the new adduct of two axially ligated canted porphyrins [Ru(TPP)(CO)(3'MPyP)] (**1**) (TPP = tetraphenylporphyrin, 3'MPyP = 5-(3'-pyridyl)-10,15,20-triphenylporphyrin) as well as its thorough spectroscopic characterization in solution, including the dynamic ¹H NMR investigation of the NH tautomeric exchange process. **1** crystallizes in the monoclinic space group *P*2₁/*a*, *Z* = 4, with *a* = 13.508(1) Å, *b* = 29.972(1) Å, *c* = 19.084(1) Å, and β = 96.03(1)°. The structural and spectroscopic data of **1** assume a strategic importance among axially ligated pyridylporphyrin systems, since they can be fruitfully compared to those of perpendicular analogues. The importance of a comparative investigation of the canted and perpendicular arrays of porphyrins is readily understood: it might help understanding how relevant physicochemical properties, such as photoinduced long-range electron or energy transfer processes, depend on the mutual orientation of the pigments in the 3-dimensional architecture while the other parameters in the supramolecular array (number of macrocycles, distance between them) are maintained substantially unchanged.

Introduction

Mixed *meso*-pyridyl/phenyl porphyrins (PyPs)¹ are being increasingly used as building blocks for the metal-mediated self-assembly of supramolecular arrays. By coordination of the peripheral pyridyl groups, PyPs can provide connections to as many as four metal centers belonging either to coordination compounds² or to metalloporphyrins.^{3–6} Most of the examples reported to date by us and others concern adducts of perpendicularly linked porphyrins, obtained by coordination of the 4'N-(py) groups of 4'-pyridyl/phenyl porphyrins (4'PyPs) to ruthenium,^{3,4} osmium,⁵ and zinc porphyrins⁶ with substitutionally labile axial ligands. Moreover, metallo-4'PyPs can self-assemble

in solution into linear or cyclic oligomers^{7,8} and 4'PyPs, or closely related pyridylporphyrins, have also been employed as linear or angular building blocks for the construction of molecular squares.⁹

Despite the several examples concerning the use of 4'PyPs, only very recently (and independently) did two reports describe well-characterized porphyrin adducts based on 3'-pyridyl/phenyl porphyrins (3'PyPs). Reaction of 3'PyPs with metalloporphyrins leads to the canted analogues of known perpendicular arrays of pigments obtained with 4'PyPs (Figure 1). In particular, we described the solution and solid state structure of the pentakis-(porphyrin) system (Zn·3'TPyP)[Ru(TPP)(CO)]₄,¹⁰ while Imamura's group described the solution properties of a bis- and a tris(porphyrin) adduct of canted porphyrins obtained by coordination of 3'MPyP and 3'*cis*-DPyP, respectively, to Os(OEP)(CO).¹¹ A previous example, concerning the coordination of 3'TPyP to zinc-porphyrin dimers, lacked a thorough solution or solid state characterization.¹²

Supramolecular arrays of porphyrins are investigated as models of the photosynthetic system.¹³ A comparative investigation of canted and perpendicular arrays of side-to-face porphy-

[†] Università di Trieste.

[‡] On leave from the Department of Physical Chemistry, Charles University, Hlavova 2030, Prague, Czech Republic.

[§] Sincrotrone Trieste.

- (1) Abbreviations: tetraphenylporphyrin, TPP; octaethylporphyrin, OEP; 5-(4'-pyridyl)-10,15,20-triphenylporphyrin, 4'MPyP; 5,10,15,20-tetrakis(4'-pyridyl)porphyrin, 4'TPyP; 5-(3'-pyridyl)-10,15,20-triphenylporphyrin, 3'MPyP; 5,10-bis(3'-pyridyl)-15,20-diphenylporphyrin, 3'*cis*-DPyP; 5,10,15,20-tetrakis(3'-pyridyl)porphyrin, 3'TPyP.
- (2) (a) Alessio, E.; Macchi, M.; Heath, S. L.; Marzilli, L. G. *Inorg. Chem.* **1997**, *36*, 5614–5623. (b) Yuan, H.; Thomas, L.; Woo, L. K. *Inorg. Chem.* **1996**, *35*, 2808–2817. (c) Steiger, B.; Shi, C.; Anson, F. C. *Inorg. Chem.* **1993**, *32*, 2107–2113.
- (3) Alessio, E.; Macchi, M.; Heath, S.; Marzilli, L. G. *Chem. Commun.* **1996**, 1411–1412.
- (4) Funatsu, K.; Kimura, A.; Imamura, T.; Ichimura, A.; Sasaki, Y. *Inorg. Chem.* **1997**, *36*, 1625–1635.
- (5) Kariya, N.; Imamura, T.; Sasaki, Y. *Inorg. Chem.* **1997**, *36*, 833–839.
- (6) (a) Li, M.; Xu, Z.; You, X.; Huang, X.; Zheng, X.; Wang, H. *Inorg. Chim. Acta* **1997**, *261*, 211–215. (b) Anderson, S.; Anderson, H. L.; Bashall, A.; McPartlin, M.; Sanders, J. K. M. *Angew. Chem., Int. Ed. Engl.* **1995**, *34*, 1096–1099.

- (7) Fleischer, E. B.; Shachter, A. M. *Inorg. Chem.* **1991**, *30*, 3763–3769.
- (8) (a) Funatsu, K.; Imamura, T.; Ichimura, A.; Sasaki, Y. *Inorg. Chem.* **1998**, *37*, 1798–1804. (b) Funatsu, K.; Kimura, A.; Imamura, T.; Sasaki, Y. *Chem. Lett.* **1995**, 765–766.
- (9) (a) Stang, P. J.; Fan, J.; Olenyuk, B. *Chem. Commun.* **1997**, 1453–1454. (b) Slone, R. V.; Hupp, J. T. *Inorg. Chem.* **1997**, *36*, 5422–5423. (c) Drain, C. M.; Lehn, J.-M. *J. Chem. Soc., Chem. Commun.* **1994**, 2313–2315.
- (10) Alessio, E.; Geremia, S.; Mestroni, S.; Srnova, I.; Slouf, M.; Gianferrara, T.; Prodi, A. Submitted for publication.
- (11) Kariya, N.; Imamura, T.; Sasaki, Y. *Inorg. Chem.* **1998**, *37*, 1658–1660.

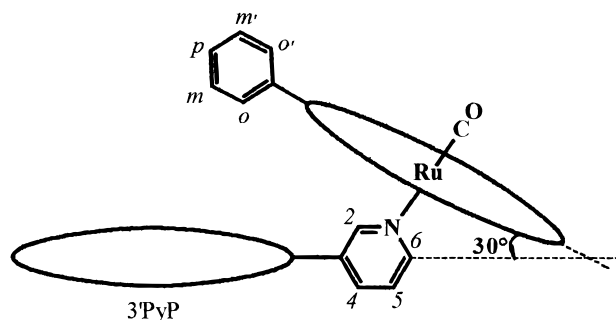


Figure 1. Schematic representations of Ru(TPP)(CO) binding to a generic 3'PyP. All phenyl rings, except one on TPP, have been omitted for clarity. The 3'N(py) and phenyl rings are assumed to lie perpendicular to the mean plane of PyP and TPP, respectively; the Ru–3'N bond is assumed perpendicular to the TPP plane.

rins might be valuable for understanding how relevant physicochemical properties, such as photoinduced long-range electron or energy transfer processes, depend on the mutual orientation of the pigments in the 3-dimensional architecture while the number of macrocycles and their distance in the supramolecular array are maintained substantially unaltered.

We report here a detailed X-ray structure of the new adduct of two axially ligated canted porphyrins [Ru(TPP)(CO)-(3'MPyP)] (**1**) as well as the spectroscopic characterization of **1** and of the corresponding zinc adduct [Ru(TPP)(CO)(Zn·3'MPyP)] (**1Zn**) in solution. The thorough structural and spectroscopic investigation of **1** assumes a strategic importance among pyridylporphyrin systems. In fact, the X-ray structure of **1** allows us to perform a direct structural comparison with the canted pentakis(porphyrin) adduct (Zn·3'TPyP)[Ru(TPP)(CO)]₄ (**2Zn**)¹⁰ and the perpendicular octaethylporphyrin system [Ru(OEP)(CO)(4'MPyP)] (**3**).⁴ The solution spectroscopic data for **1**, including the dynamic ¹H NMR investigation of the NH tautomeric exchange process, are compared with those for the perpendicular analogues **3** and [Ru(TPP)(CO)(4'MPyP)] (**4**)^{3,4} and for the canted osmium adduct [Os(OEP)(CO)(3'MPyP)] (**5**).¹¹

Experimental Section

Reagents. Analytical grade solvents and DMSO were used without further purification. All reagents, including CDCl₃ and CD₂Cl₂, were from Aldrich.

Starting Materials. [Ru(TPP)(CO)(EtOH)] was prepared according to literature methods.¹⁴ 3'MPyP was prepared according to a modified literature procedure.¹⁵ A mixture of 3-pyridinecarboxaldehyde (1.0 g, 9.3 × 10⁻³ mol), benzaldehyde (3.24 g, 3.0 × 10⁻² mol), and pyrrole (2.52 g, 3.76 × 10⁻² mol) was heated to reflux in propionic acid (120 mL) for 1 h. The mixture of 3'PyPs, which precipitated from the dark purple solution after overnight standing at room temperature, was removed by filtration, washed with cold methanol and *n*-pentane, and vacuum-dried (yield 0.54 g). 3'MPyP was separated from the other isomers by column chromatography (4.5 × 25 cm column, packed with 60 Å 230–400 mesh silica gel); tetraphenylporphyrin was removed first using chloroform as eluent, and then a 98:2 chloroform/ethanol mixture was used to elute 3'MPyP (yield 0.2 g). Characterization of 3'MPyP is as follows. ¹H NMR (CDCl₃, 400 MHz, 25 °C): 3'N(py) 9.46 (1, s, H2), 9.04 (1, m, H6), 8.52 (1, m, H4), 7.77 (1, m, H5); Hβ

Table 1. Crystallographic Data for **1**

formula	C ₈₈ H ₅₇ N ₉ ORu· 0.66CHCl ₃	<i>d</i> _{calcd} /g cm ⁻³	1.242
fw	1436.28	cryst size/mm	0.2 × 0.2 × 0.4
cryst syst	monoclinic	temp/K	100(2)
space group	<i>P</i> 2 ₁ / <i>a</i> (No. 14)	wavelength/Å	0.8
<i>a</i> /Å	13.508(1)	<i>θ</i> _{max} /deg	27.56
<i>b</i> /Å	29.972(1)	<i>h</i> , <i>k</i> , <i>l</i> range	+15,+34,±20
<i>c</i> /Å	19.084(1)	no. of independent reflins	10 811
<i>β</i> /deg	96.03(1)	<i>R</i> ₁ ^a	0.0386
<i>V</i> /Å ³	7683.6(7)	<i>wR</i> ₂ ^a	0.1194
<i>Z</i>	4	<i>S</i> ^a	1.028

^a Calculated for 9058 independent reflections with *I*₀ > 2σ(*I*₀).

8.86 (8, m); *o*-H 8.21 (6, m); *m*+*p*-H 7.77 (9, m); NH -2.78 (2, s) ppm. UV/visible spectrum (*λ*_{max}, nm (ε, M⁻¹ cm⁻¹)): in toluene solution, 419 (441 600), 483 (3700), 514 (20 100), 548 (8400), 591 (5700), 649 (4300).

[Ru(TPP)(CO)(3'MPyP)] (1**).** Addition of a stoichiometric amount of 3'MPyP (67 mg, 0.1 mmol) to a chloroform suspension of [Ru(TPP)(CO)(EtOH)] (81 mg, 0.1 mmol) yielded a deep-purple solution within minutes. The system was allowed to react overnight at room temperature. The crude product precipitated from the concentrated solution upon addition of *n*-hexane and was collected on a filter, washed with cold methanol and *n*-hexane, and vacuum-dried; yield 100 mg (70%). Recrystallization from chloroform/*n*-hexane yielded crystals suitable for X-ray analysis. Anal. Calcd for C₈₈H₅₇N₉ORu·^{1/2}CHCl₃ (*M*_r 1417.23): C, 74.9; H, 4.09; N, 8.89. Found: C, 75.1; H, 4.11; N, 8.94. Mp: > 300 °C. ¹H NMR (CDCl₃, 400 MHz, 25 °C): Hβ_{3'MPyP} 8.85 (4, m, β₃₊₄), 8.55 (2, d, β₂), 6.72 (2, d, β₁); Hβ_{TPP} 8.56 (8, s); *o*-H_{TPP} 8.21 (4, d, exo), 7.41 (4, d, endo); *m*-H_{TPP} 7.66 (4, m, exo), 7.06 (4, m, endo); *p*-H_{TPP} 7.56 (4, m); *o*-H_{3'MPyP} 8.21 (2, br), 8.14 (2, br), 8.03 (2, d); *m*-H_{3'MPyP} 7.70 (2, m, br); *m*+*p*-H_{3'MPyP} 7.79 (7, m, br); 3'N(py) 7.04 (1, m, H4), 5.68 (1, m, H5), 2.36 (1, s, H2), 1.98 (1, m, H6); NH -3.11 (2, s) ppm. IR (Nujol): ν = 1950 cm⁻¹ (C=O). UV/visible spectrum (*λ*_{max}, nm (ε, M⁻¹ cm⁻¹)): in toluene solution, 412 (420 600), 420 (423 700), 521 (29 400), 531 sh (27 400), 551 sh (14 200), 591 (6300), 649 (4400).

[Ru(TPP)(CO)(Zn·3'MPyP)] (1Zn**).** A methanol solution (3 mL) of zinc acetate (54 mg, 0.25 mmol) was added to the deep-purple chloroform solution (7 mL) of **1** (70 mg, 4.9 × 10⁻² mmol). The system was allowed to react overnight at room temperature. The crude product precipitated from the concentrated solution upon addition of *n*-hexane and was collected on a filter, thoroughly washed with methanol and then with *n*-hexane, and vacuum-dried; yield 58 mg (80%). **1** was recrystallized from chloroform/*n*-hexane. Anal. Calcd for C₈₈H₅₅N₉ORuZn (*M*_r = 1420.91): C, 74.4; H, 3.90; N, 8.87. Found: C, 74.2; H, 3.90; N, 8.83. Mp: > 300 °C. ¹H NMR (400 MHz, CDCl₃, 25 °C): Hβ_{3'MPyP} 8.95 (4, m, β₃₊₄), 8.66 (2, d, β₂), 6.81 (2, d, β₁); Hβ_{TPP} 8.54 (8, s); *o*-H_{TPP} 8.20 (4, d, exo), 7.37 (4, d, endo); *m*-H_{TPP} 7.65 (4, m, exo), 7.03 (4, m, endo); *p*-H_{TPP} 7.54 (4, m); *o*-H_{3'MPyP} 8.20 (2, br), 8.16 (2, m), 8.04 (2, d); *m*-H_{3'MPyP} 7.69 (2, m, br); *m*+*p*-H_{3'MPyP} 7.79 (7, m); 3'N(py) 7.04 (1, m, H4), 5.68 (1, m, H5), 2.32 (1, s, H2), 1.98 (1, m, H6) ppm. IR (Nujol): ν = 1949 cm⁻¹ (C=O). UV/visible spectrum (*λ*_{max}, nm (ε, M⁻¹ cm⁻¹)): in toluene solution, 411 (367 500), 425 (397 000), 536 (24 700), 548 (25 100), 590 (4600).

NMR Spectroscopy. ¹H NMR experiments were performed in CDCl₃ or CD₂Cl₂ at 400 MHz on a JEOL EX400 spectrometer equipped with a variable-temperature unit. Spectra were typically collected with a 6000 Hz spectral window, a 30° pulse, and 32K data points. All spectra were referenced to the signal of residual undeuterated solvent, set at 7.26 ppm for CDCl₃ and at 5.30 ppm for CD₂Cl₂.

Crystallographic Study. A summary of the crystal data and data collection and refinement is given in Table 1. A crystal of **1** (stable in air) was mounted on a glass fiber and then flash-frozen to 100 K. Data were collected at the X-ray diffraction beamline of the Elettra Synchrotron (Trieste, Italy), using the rotating-crystal method with a 0.8 Å monochromatic wavelength and a MAR 345 mm image plate with a crystal–detector distance of 100 mm, giving 0.85 Å resolution

- (12) Chernook, A. V.; Rempel, U.; von Borczyskowski, C.; Shugla, A. M.; Zenkevich, E. I. *Chem. Phys. Lett.* **1996**, *254*, 229–241.
 (13) (a) Kurreck, H.; Huber, M. *Angew. Chem., Int. Ed. Engl.* **1995**, *34*, 849–866. (b) Wasielewski, M. R. *Chem. Rev.* **1992**, *92*, 435–461.
 (14) Bonnet, J. J.; Eaton, S. S.; Eaton, G. R.; Holm, R. H.; Ibers, J. A. *J. Am. Chem. Soc.* **1973**, *95*, 2141–2149.
 (15) Little, R. G.; Anton, J. A.; Loach, P. A.; Ibers, J. A. *J. Heterocycl. Chem.* **1975**, *12*, 343–349.

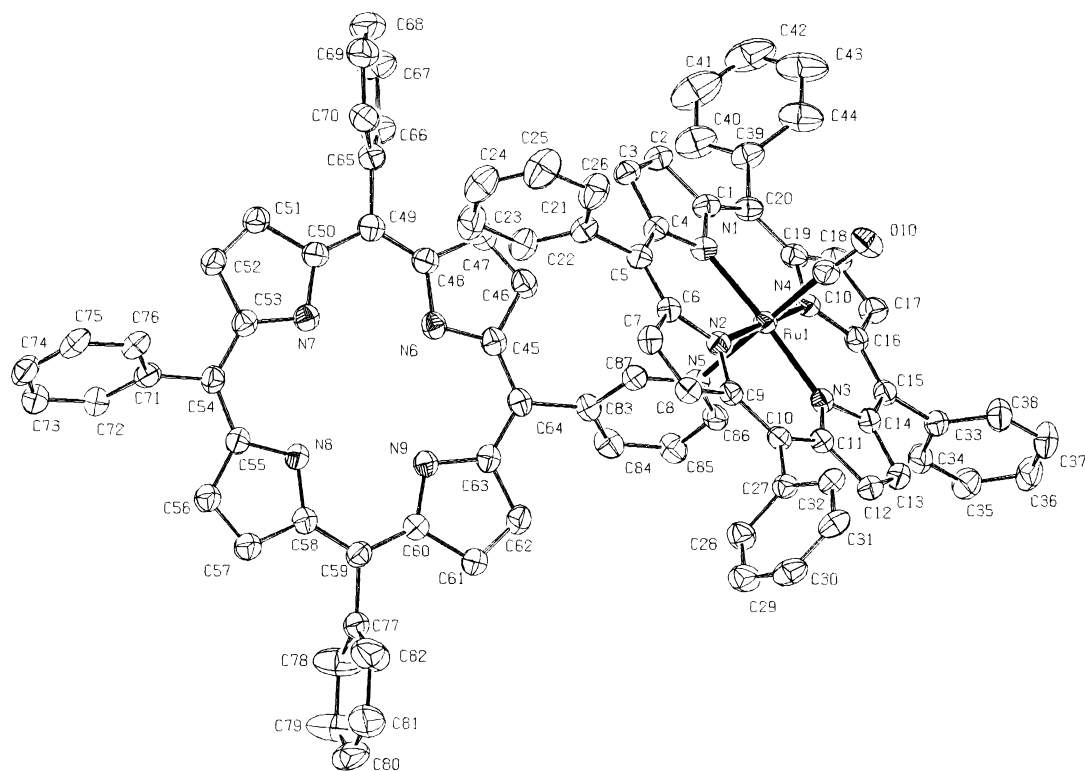


Figure 2. ORTEP view (thermal ellipsoids at 40% probability) of [Ru(TPP)(CO)(3'MPyP)] (**1**) with the atom-labeling scheme.

Table 2. Selected Bond Distances (Å) and Angles (deg) for **1**

Ru—C(CO)	1.844(3)	Ru—N3	2.059(2)
Ru—N4	2.046(2)	Ru—N5(py)	2.189(2)
Ru—N2	2.053(2)	C(CO)—O(CO)	1.146(3)
Ru—N1	2.057(2)		
N4—Ru—N1	90.35(8)	C(CO)—Ru—N1	93.81(10)
N2—Ru—N1	89.48(8)	C(CO)—Ru—N3	90.06(10)
N4—Ru—N3	89.76(8)	C(CO)—Ru—N5	175.72(9)
N2—Ru—N3	90.15(8)	N4—Ru—N5	87.49(8)
N4—Ru—N2	176.27(8)	N2—Ru—N5	88.79(8)
N1—Ru—N3	176.13(8)	N1—Ru—N5	86.70(8)
C(CO)—Ru—N4	88.26(10)	N3—Ru—N5	89.44(8)
C(CO)—Ru—N2	95.46(10)	O(CO)—C(CO)—Ru	174.4(2)

Table 3. Selected Dihedral Angles for **1** (deg)

(TPP)p—(C21—C26)p ^a	80.21(7)
(TPP)p—(C27—C32)p	78.12(6)
(TPP)p—(C33—C38)p	77.39(7)
(TPP)p—(C39—C44)p	62.07(8)
(3'MPyP)p—(C65—C70)p	62.85(9)
(3'MPyP)p—(C71—C76)p	64.26(8)
(3'MPyP)p—(C77—C82)p	86.25(12)
(TPP)p—(3'MPyP)p	43.55(2)
(TPP)p—(py)p	82.01(5)
(3'MPyP)p—(py)p	59.66(7)
(TPP)p—(3'N(py)—C84)v ^b	82.07
(TPP)p—(Ru—3'N(py))v	75.83
(py)p—(Ru—3'N(py))v	172.61

^a p = plane. ^b v = vector.

at the edge. The data were reduced using the programs DENZO¹⁶ and SCALEPACK,¹⁶ giving a final $R_{\text{merge}} = 0.040$ for 10 811 independent reflections. The structure was solved by the heavy-atom method using SHELXS-97.¹⁷ Anisotropic refinement of the complex gave an R_1 of ca. 9%. As the difference Fourier maps still showed some uninterpretable weak peaks, disordered solvent correction was made using PLATON—SQUEEZE software.¹⁸ A total of 153 electrons of disordered solvent molecules were recognized and assigned to 0.66 molecule of CHCl_3 , in agreement with elemental analysis results ($1/2 \text{CHCl}_3$). The structure was refined by full-matrix least-squares methods using SHELXL-97.¹⁷ Selected bond lengths and angles are reported in Table 2.

Results and Discussion

Molecular Structure of 1. X-ray analysis of **1** established the molecular structure shown in Figure 2. Bond distances within both porphyrin rings are average for these systems. The Ru—N(TPP) distances (Table 2) are comparable to those found in **2Zn**¹⁰ and in [Ru(OEP)(CO)(4'MPyP)] (**3**) (average 2.051 Å)⁴ and in the reference monomers [Ru(TPP)(CO)(EtOH)] (2.049-

5) Å)¹⁴ and [Ru(TPP)(CO)(py)] (2.052(9) Å).¹⁹ The Ru—3'N(py) bond length (2.189(2) Å) is comparable to those found in **2Zn** (2.179(9) Å)¹⁰ and in [Ru(TPP)(CO)(py)] (2.193(4) Å)¹⁹ but significantly shorter than that found in **3** for the 4'MPyP derivative (2.237(4) Å).⁴ Even if the comparison is not completely homogeneous, since the temperature of X-ray data acquisition for **1** and **2Zn** was 100 K and for the other structures was 298 K, this shortening of the Ru—N(py) bond length might reflect a stronger basicity of 3'PyPs compared to 4'PyPs. In any case, these distances show that the Ru—3'N(py) bond is not strained by intramolecular nonbonding interactions between the two porphyrins. Coordination of CO is almost linear, and the Ru—C(CO) bond length is comparable to those found in similar adducts.^{4,10,14,19}

The main dihedral angles of **1** are collected in Table 3 and can be directly compared to those reported for the perpendicular bis(porphyrin) adduct [Ru(OEP)(CO)(4'MPyP)] (**3**).⁴ The 3'N(py) six-membered ring forms a dihedral angle of ca. 59° with the mean plane of 3'MPyP (vs ca. 69° for 4'N(py) in **3**⁴) and of ca. 82° with the mean plane of TPP (vs ca. 63° in **3**⁴); moreover,

(16) Otwinowski, Z.; Minor, W. *Methods Enzymol.* **1997**, *276*, 307–326.

(17) Sheldrick, G. M. *SHELXL-97*, Universität Göttingen, 1997.

(18) van der Sluis, P.; Spek, A. L. *Acta Crystallogr.* **1990**, *A46*, 194–201.

(19) Little, R. G.; Ibers, J. A. *J. Am. Chem. Soc.* **1973**, *95*, 8583–8590.

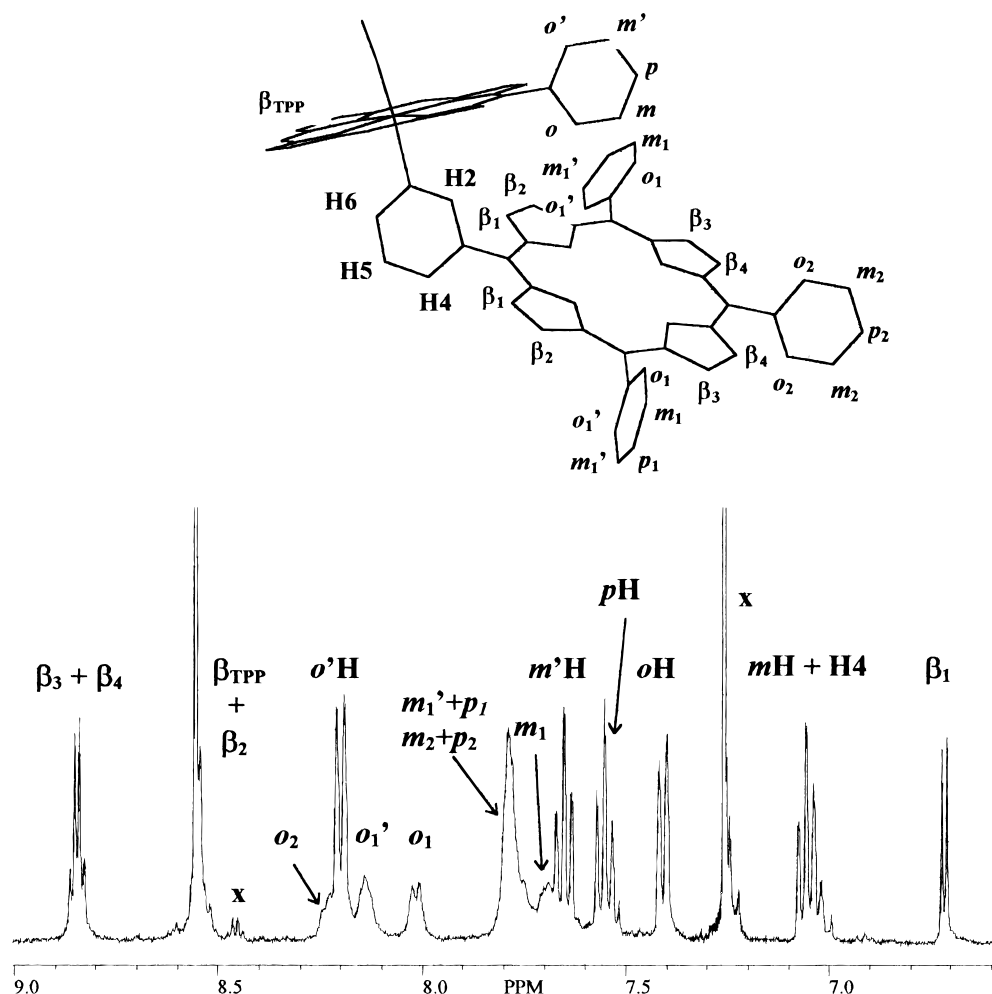


Figure 3. Downfield region of the ^1H NMR spectrum (CDCl_3 , 400 MHz) of $[\text{Ru}(\text{TPP})(\text{CO})(3'\text{MPyP})]$ (**1**). See top drawing of **1** (only one phenyl ring of TPP is reported for clarity) for the labeling scheme of the resonances. Pyrrole resonances are marked with β ; solvent peak and an impurity, with x.

the Ru–3'N(py) bond experiences a significant tilt from the perpendicular to the TPP plane (ca. 14.2° vs ca. 7.3° in **3**). As a consequence, the mutual orientation of the two porphyrins is ca. 43° (compared to ca. 40° in $(\text{Zn}\cdot 3'\text{TPyP})[\text{Ru}(\text{TPP})(\text{CO})]_4$ (**2Zn**)¹⁰ and to ca. 81° in **3**⁴). A hypothetical dihedral angle of 30° between the porphyrin planes would be expected assuming that the six-membered 3'N(py) ring lies perpendicular to the mean plane of 3'MPyP and that the Ru–3'N(py) bond is perpendicular to the TPP plane (Figure 1). The solid state distortions from this ideal arrangement are apparently removed in solution, where spectroscopic evidence agrees with a more symmetrical structure (see below).

Both porphyrins in **1** are considerably less distorted than the corresponding macrocycles in the perpendicular adduct $[\text{Ru}(\text{OEP})(\text{CO})(4'\text{MPyP})]$ (**3**).⁴ The ruthenium porphyrin is almost planar (maximum displacement is 0.059 Å for C20), and the Ru atom lies 0.0663(5) Å out of the plane toward the CO group; a larger distortion from planarity occurs in the 3'MPyP ring, with a maximum displacement of 0.162 Å (C62) out of the mean plane of the 24-atom core.

Solution Spectra. As for similar perpendicular and canted arrays of porphyrins,^{3–5,10,11} the absorption spectrum of **1** matches very closely the sum of the spectra of the monomeric components, indicating weak mutual perturbation of the chromophoric units.

The ^1H NMR spectrum of **1** in CDCl_3 solution agrees well with that reported for the OEP analogue **5**.¹¹ Both **1** and **1Zn**

are well soluble and stable (according to ^1H NMR) in chloroform solution. All signals are sharp, except those of the phenyl protons on 3'MPyP and of NH protons in **1** that are slightly broad (see below), and integration agrees well with a 1:1 ratio for TPP and 3'MPyP.

A common feature in the NMR spectra of axially ligated porphyrin arrays is the dramatic upfield shift of the resonances of the central porphyrin induced by the (cumulative) anisotropic effect of the peripheral porphyrin(s).^{3–6,10,11} This effect decreases gradually as the proton distance from the shielding macrocycle increases. In accordance with coordination of ruthenium to 3'N, in **1** the upfield shift is highest for H2 and H6 ($\Delta\delta^{20} = -7.10$ and -7.06 ppm, respectively) and decreases gradually for H5 ($\Delta\delta = -2.09$ ppm) and H4 ($\Delta\delta = -1.48$ ppm). All four phenyl rings of TPP are equivalent, indicating rapid rotation of Ru(TPP) about the Ru–3'N(py) bond; however, the pairs of *o*- and *m*-protons on each ring are clearly nonequivalent. Similar to what was observed by us for **2**,¹⁰ five well-resolved multiplets for the aromatic protons are in fact observed in the spectrum of **1** (Figure 3), with COSY connections among *o*H–*m*H–*p*H–*m'*H–*o'*H, suggesting hindered rotation about the C(*meso*)–C(phenyl) bond. In solution, the phenyl rings probably have an orientation almost perpendicular to the Ru(TPP) mean plane, similar to that found in the solid state (Table 3). Due to the

(20) The chemical shift difference $\Delta\delta$ is defined as $\delta(\text{dimer}) - \delta(\text{parent porphyrin})$.

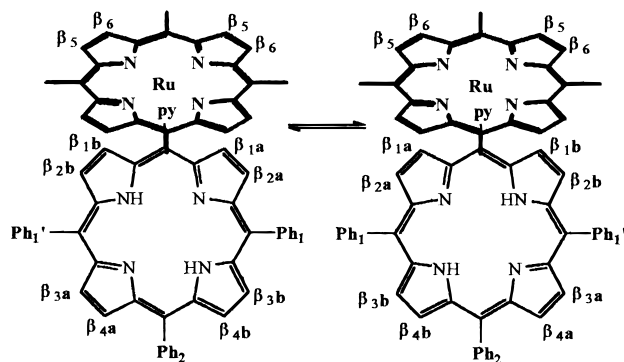


Figure 4. Schematic top view of **1** illustrating the NH-exchange equilibrium between the two degenerate tautomers. CO and phenyl rings on TPP have been omitted for clarity.

mutual orientation of porphyrin planes, which brings the phenyl rings of TPP into the anisotropic region of 3'MPyP (Figure 3), the shielding effect on endo protons (*o*H 7.41 ppm, *m*H 7.06 ppm) is much larger than that on exo protons (*o*'H 8.21 ppm, *m*'H 7.66 ppm) and considerably more pronounced than in the 4'MPyP dimers **3** and **4**.^{3,4}

The pyrrole signals of both porphyrins in **1** are consistent with the presence of a mirror plane perpendicular to the mean plane of 3'MPyP and going through the 3'N(py) ring (that must lie perpendicular to the 3'MPyP plane); this symmetry is very likely the result of rapidly (on the NMR time scale) equilibrating conformers and of the relatively fast NH tautomeric exchange process as well (see below). The two pairs of equivalent pyrrole protons of 3'MPyP closest to the ruthenium porphyrin, β H₁ and β H₂ (Figure 3), resonate as two upfield shifted doublets connected in the COSY spectrum. The remaining two pairs of equivalent pyrrole protons of 3'MPyP that are further removed from the shielding cone of Ru(TPP), β H₃ and β H₄, give an AB multiplet only slightly shifted upfield. The symmetry (in addition to fast rotation of Ru(TPP)) also makes equivalent the two sets of TPP pyrrole protons, β H₅ and β H₆ (Figure 4), and their signal is a sharp singlet. Unlike in perpendicular arrays, in **1** the pyrrole protons of TPP fall partially into the shielding cone of 3'MPyP and consequently their resonance experiences an upfield shift of ca. 0.10 ppm compared to that of uncoordinated ruthenium porphyrin and of 0.18 ppm compared to that of [Ru(TPP)(CO)-(4'MPyP)],^{3,4} where they fall into the deshielding cone of 4'MPyP.

The six *o*-H's of the phenyl rings on 3'MPyP give three well-resolved, even though broadened, multiplets integrating for two protons each. The *m*- and *p*-H's resonate as two resolved broad multiplets, integrating respectively for seven and two protons (Figure 3). Similar to the phenyls on TPP, the phenyls on 3'MPyP must experience hindered rotation about the C(*meso*)-C(phenyl) bonds and probably have an orientation almost perpendicular to the 3'MPyP mean plane. Thus, the anisotropic effect of the oblique TPP affects the endo protons of the phenyl rings more than the corresponding exo protons lying on the opposite side of 3'MPyP, in one case allowing resolution of their resonances. The most upfield shifted *o*-H₁ (8.03 ppm) and *m*-H₁ (7.70 ppm) resonances (Figure 3), connected in the COSY spectrum, were attributed to the endo protons on the two equivalent phenyl rings trans to each other. Due to the overlap of all other *m*- and *p*-H resonances, COSY connections with the exo *o*-protons of these rings (*o*-H₁') were not unambiguous. However, endo and exo protons belonging to the same phenyl are physically exchanged by its rotation about the C(*meso*)-C(phenyl) bond; thus, the *o*-H resonance at 8.14 ppm, related

to the endo *o*-H₁ resonance in a saturation transfer experiment, was safely attributed to the exo *o*-H₁' protons. The least upfield shifted (and broadest) *o*-H resonance (8.20 ppm, partially overlapped with the exo *o*-H resonance of TPP phenyls) was attributed to the ortho protons on the phenyl ring trans to the 3'N(py) ring (*o*-H₂) that, due to their removed position, were not affected significantly by the anisotropic effect of Ru(TPP).

Finally, due to the canting of the porphyrin planes, the upfield shift of the resonance of the inner NH protons in **1** ($\Delta\delta = -0.33$ ppm) is smaller compared to that observed in the corresponding orthogonal adduct **4** ($\Delta\delta = -0.46$ ppm).^{3,4}

The presence of Zn inside 3'MPyP did not significantly affect the chemical shifts of the adduct, but for a slight downfield shift (0.1 ppm) of the β H resonances of 3'MPyP, which removed the overlap between the β H₂ doublet and the pyrrole TPP singlet.

Dynamic Processes in 1. The presence of broadened resonances in the room-temperature NMR spectrum of **1** indicated the occurrence of dynamic processes, which were further investigated by VT NMR experiments.

One dynamic process concerns the rotation of the phenyl rings on 3'MPyP about the C(*meso*)-C(phenyl) bonds. We found that, upon an increase in the temperature to 45 °C, their resonances broaden further, while they sharpen at *T* below ambient, indicating that at room temperature the rate of their rotation is intermediate to slow on the NMR time scale. The slow-exchange limit of this process is reached at about 0 °C, where the resonances are rather sharp; however, for lower temperatures, the slowing of another dynamic process, the exchange of internal NH protons of 3'MPyP, induces a further splitting and broadening of such phenyl resonances (see below). The resonances of the 3'N(py) ring are always sharp between -60 and +45 °C; this experimental evidence suggests that in **1** rotation of the pyridyl ring about the C(*meso*)-C(pyridyl) bond, involving also the precession of the sterically demanding TPP macrocycle, is slow on the NMR time scale also for *T* above ambient.

It is well established that in porphyrins NH exchange occurs between two tautomers where the hydrogen atoms are bound to opposite internal N atoms;²¹ in **1**, the exchange process produces two degenerate tautomers (Figure 4). The slightly broadened NH resonance observed in the spectrum of **1** suggests that at room temperature the rate of NH exchange is close to the fast limit on the NMR time scale. Upon lowering the temperature in CDCl₃ (or CD₂Cl₂), we observed spectral changes very similar to those reported for the perpendicular osmium adduct [Os(OEP)(CO)(4'MPyP)] (**6**) in toluene-*d*₆:⁵ the NH resonance broadens further, coalesces at about -20 °C, and then splits into two equally intense, well-resolved singlets, reaching the slow-exchange limit at about -60 °C (Figure 5). As for **6**, the upfield NH resonance is attributed to the proton closest to the shielding cone of TPP.

The splitting of the NH resonance is accompanied by remarkable changes in the downfield region of the spectrum (Figure 5). When the temperature is lowered, each β H resonance of 3'MPyP first broadens and then splits into two equally intense signals, in a way very similar to that reported for 4'MPyP pyrrole signals of **6**; as for **6**, the downfield signal of each pair, β H_b, is attributed to a proton on one of the two protonated pyrrole rings,

(21) (a) Storm, C. B.; Teklu, Y. *J. Am. Chem. Soc.* **1972**, *94*, 1745-1747. (b) Gust, D.; Roberts, J. D. *J. Am. Chem. Soc.* **1977**, *99*, 3637-3640. (c) Henning, J.; Limbach, H.-H. *J. Chem. Soc., Faraday Trans. 2* **1979**, *75*, 752-766. (d) Schlabach, M.; Wehrle, B.; Limbach, H.-H.; Bunnenberg, E.; Knierzinger, A.; Shu, A. Y. L.; Tolf, B.-R.; Djerassi, C. *J. Am. Chem. Soc.* **1986**, *108*, 3856-3858. (e) Crossley, M. J.; Field, L. D.; Herding, M. M.; Sternhell, S. *J. Am. Chem. Soc.* **1987**, *109*, 2335-2341.

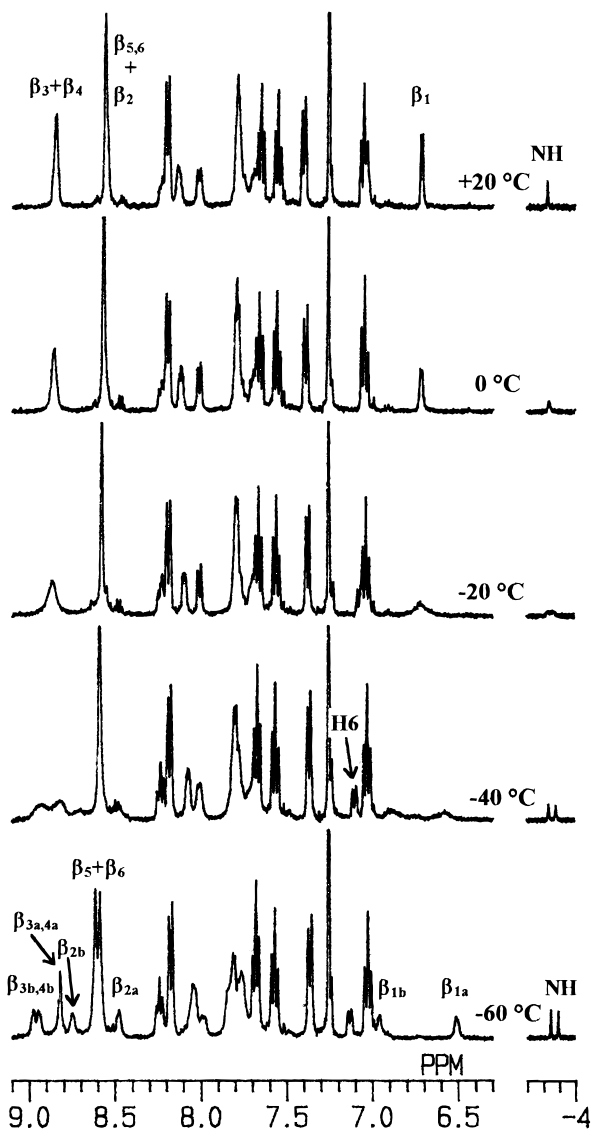


Figure 5. ^1H NMR spectra of $[\text{Ru}(\text{TPP})(\text{CO})(3'\text{MPyP})]$ (**1**) in CDCl_3 at various temperatures in the region of pyrrole proton resonances (left) and NH resonances (right).

while the upfield signal, βH_a , is attributed to the corresponding proton on the corresponding deprotonated pyrrole ring (Figure 4). At -60°C in CDCl_3 , the singlet of the pyrrole protons of TPP also splits into two equally intense resonances. In CD_2Cl_2 , where temperatures below -60°C were explored, the expected AB pattern for this pyrrole resonance was clearly detected.

The spectral changes observed upon lowering the temperature can be interpreted as follows: At room temperature the equilibrium between the two degenerate tautomers of **1** (Figure 4) is fast on the NMR time scale, thus generating the pseudomirror plane perpendicular to $3'\text{MPyP}$ and going through the $3'\text{N}(\text{py})$ ring, which divides the dimer into equivalent halves. For T close to -60°C , the equilibrium becomes slow on the NMR time scale and the pseudomirror plane is lost; accordingly, the eight pyrrole protons of $3'\text{MPyP}$ are all inequivalent as well as the two sets of TPP pyrrole protons, βH_5 and βH_6 (Figure 4). The exchange rate constants were evaluated in CD_2Cl_2 with the width at half-height of the NH resonances from -60 to -20°C ;²² rate constants based on band-shape analysis of NH resonances using the gNMR program were in good agreement

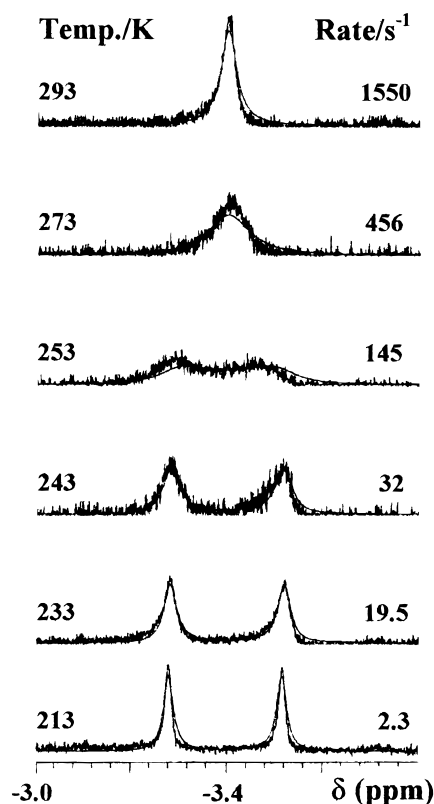


Figure 6. Experimental and computer-simulated spectra of the exchanging NH protons of $[\text{Ru}(\text{TPP})(\text{CO})(3'\text{MPyP})]$ (**1**) in CD_2Cl_2 . "Best-fit" rate constants are given for each temperature.

with those evaluated experimentally (Figure 6).²³ The Arrhenius plot afforded an activation energy, E_a , of 42.4 kJ mol^{-1} , comparable to that of 40.5 kJ mol^{-1} reported for **6** in toluene.⁵

Finally, in CD_2Cl_2 a broadening of all resonances was observed for $T < -70^\circ\text{C}$, very likely due to the decreased rate of rotation of $\text{Ru}(\text{TPP})$ about the $\text{Ru}-3'\text{N}(\text{py})$ bond.

Conclusions

The X-ray structure of $[\text{Ru}(\text{TPP})(\text{CO})(3'\text{MPyP})]$ (**1**) established that, in the solid state, the two mean porphyrin planes in **1** are canted at an angle of ca. 43° . Due to the good crystallinity and the relatively large dimensions of the crystals of **1** and to the use of the synchrotron radiation at low temperature (100 K), a high-resolution data collection was possible. The diffraction data allowed us to refine the atomic positional parameters of **1** with the lowest estimated errors (and with the best R factor) among those determined so far for similar porphyrin adducts.^{4,6,7,10}

According to NMR measurements, the solution structure of **1** is very similar to that found in the solid state though more symmetrical, due to the presence (at room temperature) of a pseudomirror plane perpendicular to $3'\text{MPyP}$ and going through the $3'\text{N}(\text{py})$ ring. At room temperature in dimer **1**, beside the relatively fast tautomeric exchange involving inner hydrogen migration in $3'\text{MPyP}$, the only other fast motion is rotation of the ruthenium porphyrin about the $3'\text{N}(\text{py})-\text{Ru}$ bond. All six-membered rings experience hindered rotation about the $\text{C}(\text{meso})-\text{C}(\text{ring})$ bond; chemical shift and symmetry considerations indicate that they are almost perpendicular to the mean plane of the corresponding porphyrin. Therefore, in solution the

(22) Sandström, J. *Dynamic NMR Spectroscopy*; Academic Press: London, 1982.

(23) Budzelaar, P. H. M. *gNMR for Windows*, Version 4.0.1; Cherwell Scientific Publishing Limited: Oxford, U.K., 1993–1997.

dihedral angle between 3'MPyP and TPP planes might be closer to the hypothetical value of 30°.

From the point of view of a detailed NMR investigation, the adducts of axially ligated canted porphyrins [Ru(TPP)(CO)-(3'MPyP)] (**1**) and (3'TPyP)[Ru(TPP)(CO)]₄ (**2**) proved to be even more valuable than the corresponding more symmetrical perpendicular systems. This is particularly true for adducts with low symmetry, such as **1**. In [Ru(TPP)(CO)(3'MPyP)], due to the mutual anisotropic shielding effect of the two porphyrins, each macrocycle acts as a powerful shift reagent on the resonances of the other, allowing resolution of signals (i.e., the phenyl resonances) and facilitating the investigation of dynamic processes such as NH tautomeric exchange.

(24) Prodi, A.; Indelli, M. T.; Kleverlaan, C. J.; Scandola, F.; Alessio, E.; Gianferrara, T.; Marzilli, L. G. *Chem.—Eur. J.*, in press.

Finally, as reported in detail elsewhere by us,²⁴ we found no appreciable differences in photophysical behavior between the bis(porphyrin) system **1** and the pentakis(porphyrin) system **2** and between canted and perpendicular analogues as well.

Acknowledgment. We thank the Italian MURST for financial support and Johnson Matthey for a loan of hydrated RuCl₃. We also thank the CNR staff at ELETTRA for help in the use of the facility supported by the CNR and by the Elettra Scientific Division. Discussion of the NMR data with Professor Luigi G. Marzilli (Emory University, Atlanta, GA) is gratefully acknowledged.

Supporting Information Available: An X-ray crystallographic file in CIF format. This material is available free of charge on the Internet at <http://pubs.acs.org>.

IC980816P